Available online at www.sciencedirect.com
SCIENCE DIRECT
Journal of Photochemistry and Photobiology A: Chemistry 181 (2006) 60–66
Journal of Photochemistry and Photobiology A:Chemistry
www.elsevier.com/locate/jphotochem

# Interaction mechanism in pyrromethene dye/photoacid generator photosensitive system for high-speed photopolymer

Shota Suzuki [a,b], Xavier Allonas [a,*], Jean-Pierre Fouassier [a], Toshiyuki Urano [c], Shigeru Takahara [b], Tsuguo Yamaoka [b]

[a] *Département de Photochimie Générale, Ecole Nationale Supérieure de Chimie de Mulhouse, 3 Rue Alfred Werner, 68093 Mulhouse, France*
[b] *Department of Information and Image Science, Faculty of Engineering, Chiba University, 1-33 Yayoi-cho, Inage-ku, Chiba 263-8522, Japan*
[c] *MCC-Group Science & Technology Research Center, 1000 Kamoshida-cho, Aoba-ku, Mitsubishi Chemical Corporation, Yokohama 227-8502, Japan*

Received 2 October 2005; received in revised form 27 October 2005; accepted 28 October 2005
Available online 7 December 2005

**Abstract**

The sensitization mechanism of a photoacid generator (PAG), *N*-(trifluoromethanesulfonyloxy)-1,8-naphthalimide (NIOTf) by a pyrromethene sensitizing dye, such as 1,3,5,7,8-pentamethyl pyrromethene $BF_2$ complex (HMP), 2,6-diethyl-1,3,5,7,8-pentamethylpyrromethene $BF_2$ complex (EMP), and 2,6-diethyl-8-phenyl-1,3,5,7-tetramethylpyrromethene $BF_2$ complex (EPP), was studied by means of absorption and fluorescence spectroscopies, product analysis and nanosecond laser flash photolysis. For all the systems pyrromethene/NIOTf, the fluorescence quenching was nearly diffusion-controlled. This reaction involves an electron-transfer process from the excited singlet state of the pyrromethene derivative to NIOTf, as supported by the negative values of the Gibbs free energy change and the observation of the pyrromethene radical cations. The triplet state of the pyrromethene dyes was found to be unreactive toward NIOTf. Photoacid generation quantum yields for the sensitization were also measured and they showed a correlation with the electron-transfer rate constant from the dye singlet excited state. Finally, the system EPP/NIOTf was applied to printing technology with an appropriate binder polymer bearing an acetal protection group. By controlling the exposure energy and the post-exposure baking (PEB) process, a printing plate was obtained with a high resolution.


*Keywords:* Pyrromethene dye; Photoacid generator; *N*-(Trifluoromethanesulfonyloxy)-1,8-naphthalimide; Sensitization mechanism; CTP

## 1. Introduction

Visible laser direct imaging technologies play an important role, especially in the field of printing. Production of printing plates by a scan-exposure is one of the key technologies today, since the process is drastically simplified compared to the conventional technology which requires a transparent film for the corresponding image and a flood-exposure of a photosensitive layer through the film. The research has been mainly focused on highly photosensitive initiating systems for violet laser diode (405 nm), argon ion laser (488 nm, 514.5 nm), and FD-YAG laser (532 nm). The concept of photoinduced free radical polymerization has been widely applied for negative printing plates [1–3] and the photosensitive layer is mainly composed of a sensitizing dye, a radical generator, an acrylate monomer, and alkali-soluble binder polymer. The great advantage of the radical polymerization is to allow a large choice for the sensitizing dyes, such as the well-established cyanine or coumarin derivatives, and additionally, the photogenerated radicals are highly reactive toward acrylate monomers [2,3]. Nevertheless, the major drawback is that the radicals easily react with oxygen, and a gas barrier layer should be coated on the photosensitive layer to avoid the inhibition of the polymerization [2].

In order to circumvent this problem, positive plates can be used that do not require radical polymerization. Recently, novel visible laser initiating systems, for used in positive plates, have been already tested in terms of photosensitivity of the photosensitive layer [4,5]. These systems were based on the concept of chemical amplification developed in the field of photoresist [6,7] using a photoacid generator (PAG). The best photosensitivity data was obtained using the system 2,6-diethyl-8-phenyl-1,3,5,7-tetramethylpyrromethene $BF_2$ complex (EPP)/*N*-(trifluoromethanesulfonyloxy)-1,8-naphthalimide (NIOTf) which yields a value of 0.098 mJ/cm$^2$: this value is considered as

* Corresponding author. Tel.: +33 389 336874; fax: +33 389 336895.
*E-mail addresses:* shota_szk@ybb.ne.jp (S. Suzuki), x.allonas@uha.fr (X. Allonas).

1010-6030/$ – see front matter © 2005 Elsevier B.V. All rights reserved.
doi:10.1016/j.jphotochem.2005.10.035

extremely high and competitive with those obtained in conventional radical polymerization systems.

NIOTf is a representative photoacid generator extensively used in the field of photoresist. The mechanism of photoacid generation through direct excitation of NIOTf has been studied by means of absorption and fluorescence spectroscopy methods and laser flash photolysis. It seems that a heterolytic cleavage of the weakest N–O bond takes place upon photolysis of NIOTf, as shown by the detection of *N*-hydroxynaphthalimide as the final product [8]. By contrast, the sensitization of photoacid generators by dyes has been less studied than that of the radical generators [4,5,9]. One of the reasons might be that the photogenerated acids can be partly neutralized by the heterocycles bearing a nitrogen atom or amines in the structures of the sensitizing dyes [5,10].

Pyrromethene dyes appear as potential candidates for the sensitization of various active species generators such as NIOTf. However, although a large number of reports have been proposed about synthesis [11–15], photophysical properties [16–21], photostability [19–23], applications to holography [24], electroluminescence material [25], and photopolymers [26], there are not a great deal with the sensitization of photoacid- or photobase-generators by these family of dyes.

In the present study, we investigated the sensitization mechanism for the pyrromethene/NIOTf system. The direct observation of the reaction intermediates was possible and the main factors that affect the acid generation are discussed. Finally, an example of application to printing technology without any over-coating layer was carried out, resulting in a high-resolution printing plate.

## 2. Experimental

The pyrromethene derivatives, 1,3,5,7,8-pentamethyl pyrromethene $BF_2$ complex (HMP), 2,6-diethyl-1,3,5,7,8-pentamethylpyrromethene $BF_2$ complex (EMP), and 2,6-diethyl-8-phenyl-1,3,5,7-tetramethylpyrromethene $BF_2$ complex (EPP) were synthesized as described in the literature [12,13]. The photoacid generator used was *N*-(trifluoromethanesulfonyloxy)-1,8-naphthalimide (NIOTf) as provided by Midorikagaku, and recrystallized twice from chloroform prior to use (Scheme 1).

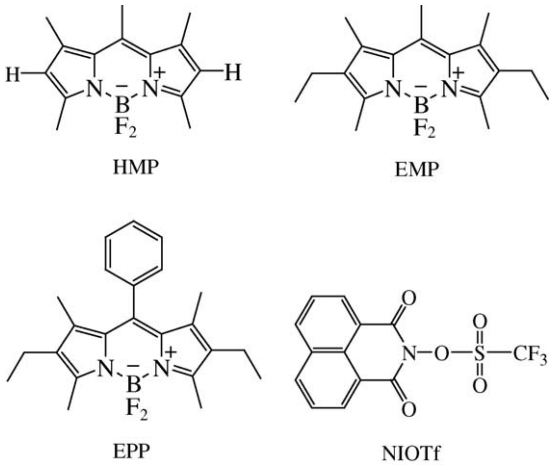


Scheme 1.

Ground-state absorption and fluorescence spectra were recorded on a Beckman DU640 spectrophotometer and a Jobin Yvon FluoroMax 2 fluorescence spectrophotometer, respectively. Fluorescence lifetimes were measured using a pulsed LED emitting at 457 nm together with a pulsed diode controller (PDL-800-B, Picoquant) operating at 10 MHz for excitation source. The detection was made using a fast photomulplier (H5783P-04, Hamamatsu) and a single photon counting setup (Fluotime 100 and Timeharp 200, Picoquant). The response function was lower than 0.7 ns and a classical procedure of iterative deconvolution was applied. All the fluorescence experiments were performed in acetonitrile under argon bubbling.

The redox potentials were measured by cyclic voltammetry using a potentiostat (Princeton Applied Research 263A) at a scan rate of 1 V/s. All compounds were dissolved in Ar-saturated acetonitrile (Fluka, spectroscopic grade) containing 0.1 M of tetrabutylammonium hexafluorophosphate (Fluka, electrochemical grade) as the supporting electrolyte. The working electrode was a vitreous carbon electrode (3 mm diameter). A saturated calomel electrode in methanol was used as a reference, its potential being controlled using the standard ferrocene/ferricinium redox couple. All redox potentials were estimated from half-peak potentials.

Time-resolved laser spectroscopy experiments were carried out by using an excitation source based on a nanosecond Nd:YAG laser (Powerlite 9010, Continuum) that operates at 10 Hz, and includes an injection seeding system improving the shot to shot stability. The frequency is doubled and the 532 nm output beam can be used to irradiate the sample after attenuation. The output laser beam can also be tripled and used to pump an optical parametric oscillator (Sunlite, Continuum) and a frequency-doubling system (FW-1, Continnum) allowing to produce any exciting wavelength from 225 nm to 1800 nm. Time-resolved absorption spectroscopy was achieved using a commercial pulsed spectrophotometer (LP900, Edinburgh Instruments).

High performance liquid chromatography (HPLC) was carried out using a three-line degasser (JASCO, DG-980-50), a solvent mixing module (HG-980-31), an HPLC pump (PU-980), a multi wavelength detector (MD-915), and an Inertsil ODS-3 column (GL Science Inc., 5 μm, 4.6 mm × 250 mm).

Photoacid generation quantum yield ($\phi_{acid}$) was determined by a spectrophotometric method using the sodium salt of tetrabromophenol blue (TBPBNa, Aldrich) as an acid sensor [27]. For the measurement, the pyrromethene derivative and NIOTf are dissolved in acetonitrile, and irradiated by the OPO system at a wavelength where NIOTf does not absorb (500 nm). The absorbed light energy ($E_{abs}$) is given by the following equation:

$$E_{abs} = I_0 \int_0^T (1 - 10^{-A(t)})\,dt$$
$$A(t) = \varepsilon_{500} C(t) l \quad (1)$$

where $I_0$ is the light intensity of the laser (mJ/pulse), $\varepsilon_{500}$ the molar extinction coefficient of the pyrromethene derivative at 500 nm, $C(t)$ the concentration of the pyrromethene derivative

at each irradiation time (i.e. the number of the laser shots), and $l$ the optical path length of the quartz cell (1 cm). The laser energy was fixed to 6.8 mJ/pulse. Then, TBPBNa is added to the cell and the subsequent bimolecular reaction between TBPBNa and the photogenerated acid is monitored at the maximum absorbance of TBPBNa (615 nm). All the quantum yields were corrected by the value corresponding to 100% of the dye fluorescence quenching.

For the application to printing technology, a terpolymer based on 2-methyl-1-propyloxypropyl methacrylate, methylmethacrylate and 2-hydroxyethylmethacrylate (P-8003) ($M_w$ = 12,500, $M_w/M_n$ = 2.2, acid value = 80, $T_g$ = 90 °C), was provided by Kyowa Hakko Chemical. P-8003 was dissolved in cyclohexanone (18% by weight of solids) with the system EPP/NIOTf (P-8003:EPP:NIOTf = 100:1:5 in weight). The photopolymer solution was spin-coated on a grained aluminium plate and baked at 100 °C for 5 min (1.1 μm thickness), followed by exposure using the argon ion laser (514.5 nm, 1.2 mJ/cm$^2$ s, Spectra Physics, Model 2016), through a screen tint or an imaging chart (Kodak). Then the PEB process was applied for the purpose of acid diffusion at 120 °C and different times. Finally, the photosensitive layer was developed in a 2.38 wt% aqueous solution of tetramethylammonium hydroxide (TMAH) and isopropyl alcohol combined in a weight ratio of 7:3 for 90 s. A developing ink (Fuji film, PS developing ink PI-2) was coated to clearly see the image obtained by using the imaging chart. A dot profile was observed by a laser microscope (Keyence, VK-8500/8510).

## 3. Results and discussion

### 3.1. Photophysical properties of the pyrromethene derivatives

Absorption spectra of HMP, EMP, and EPP are reported in Fig. 1. The $S_0$–$S_1$ transition occurs in the green with high-extinction coefficients. EMP and EPP exhibit a red shift compared to HMP due to the presence of the ethyl group (electron-releasing substituent) at the 2 and 6 positions of the pyrromethene chromophore (Fig. 1). In addition, compared to EMP, EPP exhibits a slight red shift (6 nm) because of the introduction of the phenyl group (electron-withdrawing substituent) at the 8 position that undergoes an increase of the electron-charge density in the excited state [20,21]. The fluorescence quantum yield ($\phi_f$) of EPP was determined using EMP in acetonitrile as a standard [18]. It was found that all the three compounds exhibit high fluorescence quantum yields. Small differences in the fluorescence quantum yields of EPP compared to the literature likely arise from the choice of a different fluorescent standard.

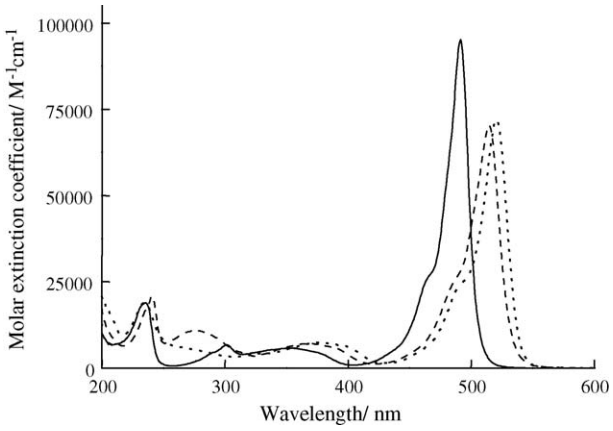


Fig. 1. Ground-state absorption spectra of HMP (solid), EMP (broken), and EPP (dotted) in acetonitrile.

From redox potentials, it was found that HMP, EMP, and EPP have similar electro-donating properties. All the relevant photophysical properties, together with the electrochemical data, are summarized in Table 1.

### 3.2. Steady-state photolysis and acid generation

Addition of NIOTf to pyrromethene dyes solution does not lead to any charge-transfer complex. The change in the ground-state absorption spectra of EPP in the EPP/NIOTf system upon laser irradiation at 500 nm is shown in Fig. 2a. The decrease in the EPP absorbance was observed when increasing the exposure energy. In control experiments, no spectral changes of the pyrromethene derivatives themselves were observed upon the laser irradiation, and besides, the pyrromethene derivatives did not decompose under addition of acids. Therefore, it is clear that the decomposition of the pyrromethene derivatives originated from the photochemical reaction with NIOTf. The photolysis quantum yields of each dye ($\phi_{ph}$) are summarized in Table 2.

Fig. 2b shows the important decrease of the absorbance of the acid sensor (TBPBNa) added to a photolysed solution of EPP/NIOTf. This allows to confirm that the interaction of NIOTf with the excited states of the pyrromethene dyes results in the generation of acids. In control experiments, and under direct excitation of NIOTf at 355 nm, a quantum yield of 0.18 was obtained by applying this method, in good agreement with that reported by Ortica et al. (0.17) [8]. Therefore, the photoacid

Table 1
Photophysical and electrochemical properties of the pyrromethene derivatives

| | $\lambda_{max}$ (nm) | $\lambda_{max}^{EM}$ (nm) | $\varepsilon_{max}$ ($M^{-1}$ $cm^{-1}$) | $E_s$ (kcal/mol) | $\tau_f$ (ns) | $\varphi_f$ | $E_T$[a] (kcal/mol) | $\tau_T$ (μs) | $E_{ox}$ (V/SCE) | $E_{red}$ (V/SCE) |
|---|---|---|---|---|---|---|---|---|---|---|
| HMP | 492 | 506 | 95100 | 57.4 | 6.0 | 0.93[b] | –[c] | –[c] | 1.21 | −1.18 |
| EMP | 515 | 536 | 70400 | 54.6 | 6.8 | 0.85[d] | 40.2 | 33 | 1.07 | −1.24 |
| EPP | 521 | 538 | 72000 | 54.0 | 5.8 | 0.77 | 37.5 | 39 | 1.10 | −1.16 |

[a] Determined according [17].
[b] From [20].
[c] Not observed.
[d] From [18].

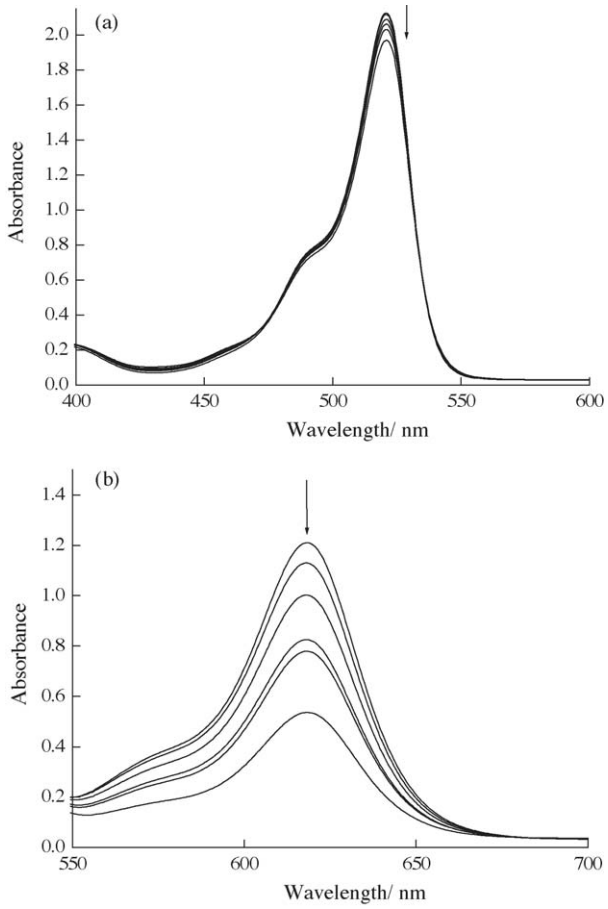


Fig. 2. (a) Steady-state photolysis of EPP ($3.11 \times 10^{-5}$ mol/l) in the EPP/NIOTf system at different irradiation times (from 0 J/cm$^2$ to 1.9 J/cm$^2$). [NIOTf] = $2.44 \times 10^{-2}$ mol/l. (b) Decrease in the absorption spectra of the TBPBNa acid sensor in the EPP/NIOTf system. [EPP] = $3.11 \times 10^{-5}$ mol/l, [NIOTf] = $2.44 \times 10^{-2}$ mol/l, [TBPBNa] = $1.69 \times 10^{-4}$ mol/l.

quantum yields ($\phi_{acid}$) can be safely determined by this method. The results are summarized in Table 2. The values obtained are low and in the range of 1–2%. Interestingly, the $\phi_{acid}$ values are higher than $\phi_{ph}$ for all the systems studied. This suggests that the pyrromethene dye is partly recovered during the photochemical process. In a 1:1 mixture of acetonitrile and isopropanol, the $\phi_{acid}$ value for the HMP/NIOTf system increases up to 0.053, as a consequence of the presence of a protic solvent.

Table 2
Fluorescence quenching rate constants, Gibbs free energy changes, quantum yields of acid generation and dye photolysis for each pyrromethene/NIOTf system

| | HMP | EMP | EPP |
|---|---|---|---|
| $\log k_q^S$ | 10.1 | 10.2 | 9.96 |
| $\log k_q^T$ | –[a] | 6.21 | 5.93 |
| $\Delta G_S$[b] (kcal/mol) | −7.6 | −8.1 | −6.8 |
| $\Delta G_T$[b] (kcal/mol) | –[a] | 6.3 | 9.7 |
| $\phi_{acid}$[c] | 0.017 | 0.008 | 0.011 |
| $\phi_{ph}$[c] | 0.006 | 0.003 | 0.004 |

[a] Triplet state not observed.
[b] $E_{red}$ of NIOTf is −0.95 V/SCE.
[c] Corrected for 100% fluorescence quenching.

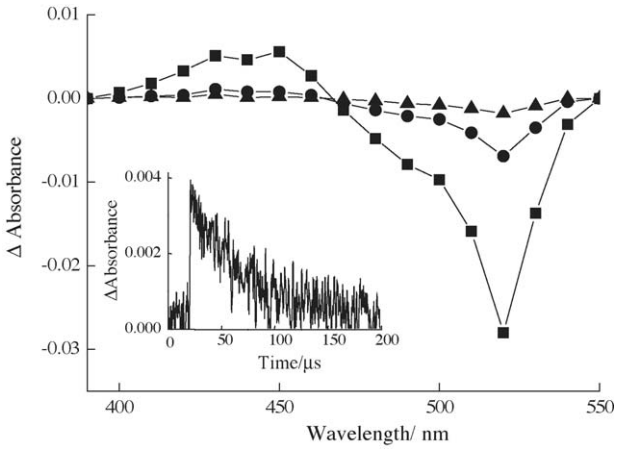


Fig. 3. Transient absorption spectra of EPP observed 3 μs (square), 80 μs (circle), and 180 μs (triangle) after the laser pulse (532 nm, 5 mJ/pulse). Inset: decay kinetics monitored at 440 nm. [EPP] = $1.77 \times 10^{-5}$ mol/l.

### 3.3. Excited-state study

As pyrromethene derivatives have high fluorescence quantum yields, it is suggested that the bimolecular reaction between the pyrromethene derivative and NIOTf mainly takes place from the excited singlet state. Indeed, under addition of NIOTf in acetonitrile, it was found that the fluorescence intensity of pyrromethene dyes decreases. Fluorescence quenching rate constants ($k_{qs}$) were determined for all the pyrromethene derivatives by using the Stern–Volmer equation and are summarized in Table 2. They are close to the diffusion-controlled rate constant in acetonitrile.

Laser excitation of pyrromethene dyes results in transient absorption spectra, as reported in Fig. 3 for EPP. A negative transient absorption was observed around 530 nm that corresponds to the bleaching of the pyrromethene ground state. A positive transient absorption was observed in the range of 400–450 nm that exhibits both a spectral profile and a decay time very similar to those reported for the triplet state of EMP [17,18]. Energy transfer experiments using perylene as a donor confirm this attribution for both EMP and EPP. By the way, the triplet–triplet equilibrium between the pyrromethene dye and perylene allows a determination of the triplet energy of the dye according to a procedure described in the literature [17]. The measured triplet energy was found to be 40.2 kcal/mol for EMP, in good agreement with the published value of 37.5 kcal/mol [17]. The same procedure leads to a value of 40.2 kcal/mol for EPP

Under the addition of NIOTf, no significant change was observed in the triplet state lifetime of EPP. The calculated interaction rate constant is negligibly low (Table 2), indicating that no interaction takes place between the triplet state of the dye and the NIOTf ground state. The triplet state of HMP was not observed under our experimental conditions.

### 3.4. Interaction mechanism

The values of the Gibbs free energy change for the photoinduced electron transfer from the singlet ($\Delta G_S$) or the triplet ($\Delta G_T$) state of each dye to NIOTf were determined by the

Rehm–Weller equation [28]:

$$\Delta G_{S,T}\,(\text{kcal/mol}) = 23.06(E_{ox} - E_{red}) - E_{S,T}$$

where $E_{ox}$ and $E_{red}$ are the oxidation and reduction potentials of the pyrromethene derivative and NIOTf, respectively. $E_S$ and $E_T$ stand for the excitation energy of each pyrromethene derivative in the singlet or triplet state, respectively. All the $\Delta G_S$ values are negative, indicating that an exergonic singlet electron transfer can take place in all the systems (Table 2). Concerning the reaction from the triplet state, all the $\Delta G_T$ values are positive, indicating that the process is not exergonic enough to be operative. Therefore, the fluorescence quenching of pyrromethene dyes is explained on the basis of a photoinduced electron transfer from the singlet excited dye to the NIOTf ground state. On the contrary, the absence of triplet-state quenching is confirmed by the positive value of $\Delta G_T$.

The radical cation of the pyrromethene derivative or the radical anion of NIOTf was expected to be formed from the electron-transfer reaction. Nanosecond laser flash photolysis was carried out in order to detect some possible reaction intermediates. In the case of the system EPP/NIOTf, a new long-lived transient species was detected from 390 nm to 420 nm (Fig. 4) in addition to that of the EPP triplet state. The absorption spectrum of the EMP radical cation was already observed during the interaction of EMP with a pyromellitic dianhydride [18]. Although the reported lifetime was shorter than in our case, the spectral profile matches quite well the one observed by us

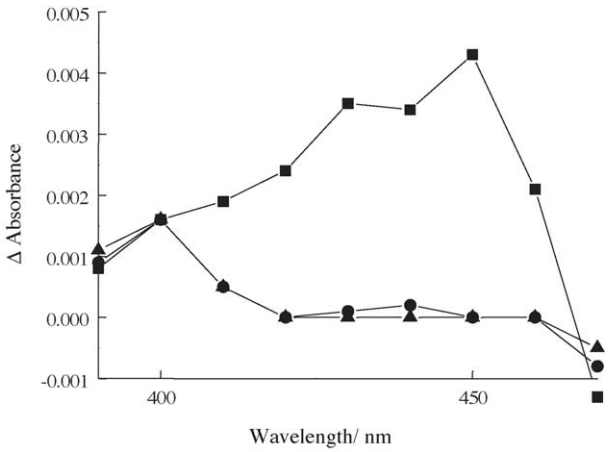


Fig. 4. Transient absorption spectra obtained from the EPP/NIOTf system observed 3 μs (square), 80 μs (circle), and 180 μs (triangle) after the laser pulse (532 nm, 5 mJ/pulse). [EPP] = $1.77 \times 10^{-5}$ mol/l, [NIOTf] = $1.21 \times 10^{-2}$ mol/l.

for the EPP/NIOTf system (Fig. 4). This allows the attribution of the long-lived species at 400 nm to the radical cation of EPP.

The concentration dependence of NIOTf on the decay kinetics for the system EPP/NIOTf was studied as shown in Fig. 5. The optical density of the radical cation monitored at 400 nm increases with increasing NIOTf concentration, as shown in Fig. 5a. Concomitantly, the ground-state bleaching of EPP as monitored at 520 nm exhibits the same tendency (Fig. 5b).

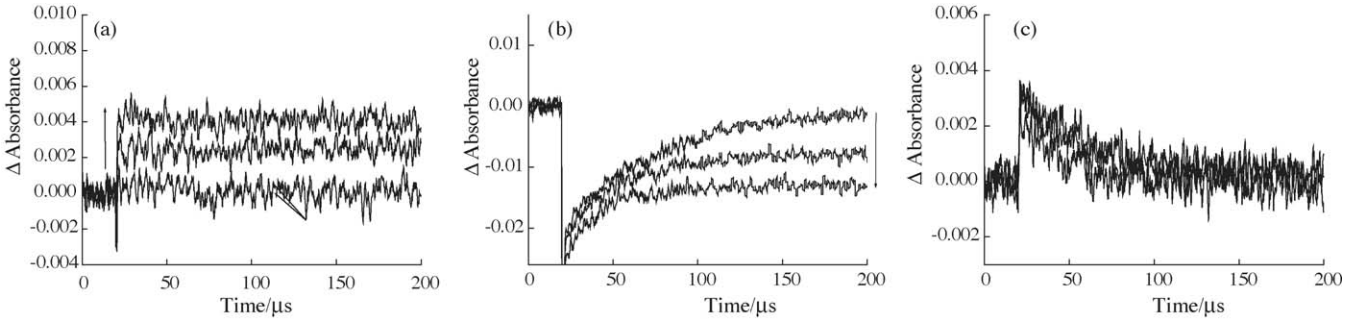


Fig. 5. Concentration dependence of NIOTf on the decay kinetics for the EPP/NIOTf system, monitored at: (a) 400 nm, (b) 520 nm, and (c) 440 nm. [EPP] = $1.77 \times 10^{-5}$ mol/l, [NIOTf] = 0–$2.41 \times 10^{-2}$ mol/l.

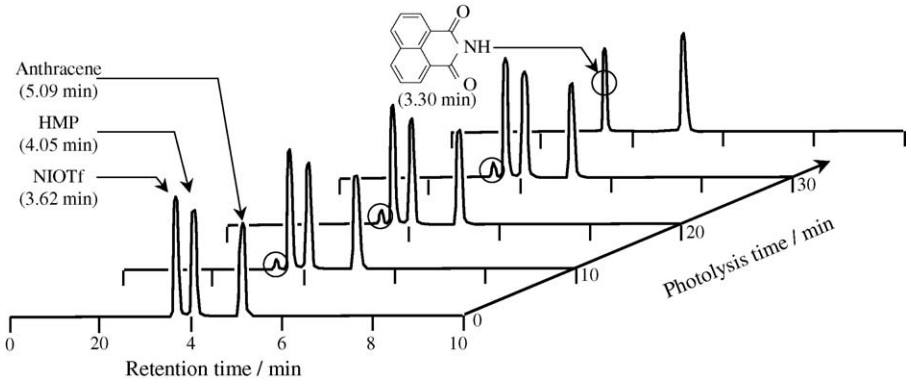


Fig. 6. HPLC chromatograms obtained on photolysed solutions of EPP/NIOTf in acetonitrile at different irradiation times.

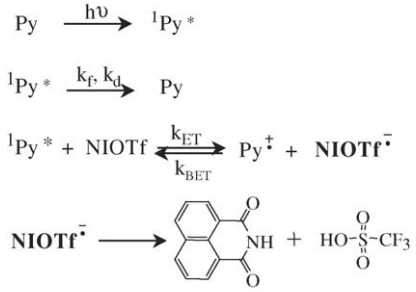


Scheme 2.

Finally, the triplet state observed at 440 nm was not affected by the increasing concentration of NIOTf (Fig. 5c). On the basis of these observations, we concluded that singlet electron transfer takes place in the pyrromethene derivative/NIOTf systems.

HPLC and mass spectrometric analysis were carried out in acetonitrile to determine the final product upon photolysis by the argon ion laser. As the irradiation time became longer, the formation of 1,8-naphthalimide was observed, as confirmed by the retention time (Fig. 6), the absorption and mass spectra of the authentic sample. By analogy to the behaviour of *N*-acyloxyphtalimide [29], it is proposed that 1,8-naphthalimide was formed from the radical anion of NIOTf. These experiments allows to propose a mechanism for the acid generation involving an interaction between the first excited singlet state of the pyrromethene dye and NIOTf (Scheme 2). In this scheme, $k_f$, $k_d$, $k_{ET}$, and $k_{BET}$ represent the rate constants of fluorescence, deactivation, electron transfer, and returned electron transfer, respectively. The reducing agent is expected to be water in the polymeric media as well as in net acetonitrile that contains about 20 ppm of residual water [8].

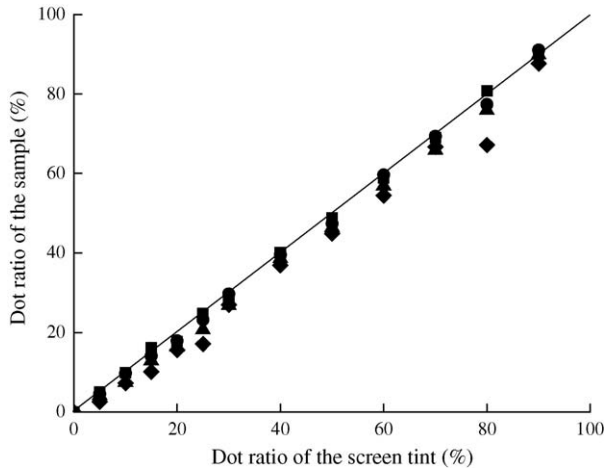


Fig. 7. Relationship between the dot ratio of the screen tint and that of the developed sample at different exposure energies: 0.82 (square); 2.46 (circle); 4.92 (triangle); 7.38 (rhombus) mJ/cm$^2$, together with 45° ideal line. PEB 2 min.

### 3.5. Application to printing technology

Attempt was made to apply the EPP/NIOTf system to printing technology using the binder polymer bearing the acetal protection group (P-8003). In this system, the acid-catalyzed deprotection of the binder polymer is induced and the alkali developer insoluble polymer is converted to a soluble one only in the exposed area. During this process, a carboxylic acid is generated that renders the polymer alkali soluble. Scheme 3 describes the two possible mechanisms that account for this process, although it is out of the scope of this paper to decipher between them [30].

The relationship between the dot ratio of the screen tint (65 lpi) and that of the developed printing plate was investigated as a function of the exposure energy from 0.82 mJ/cm$^2$ to 7.38 mJ/cm$^2$ (Fig. 7). The dot size shrunk when increasing the

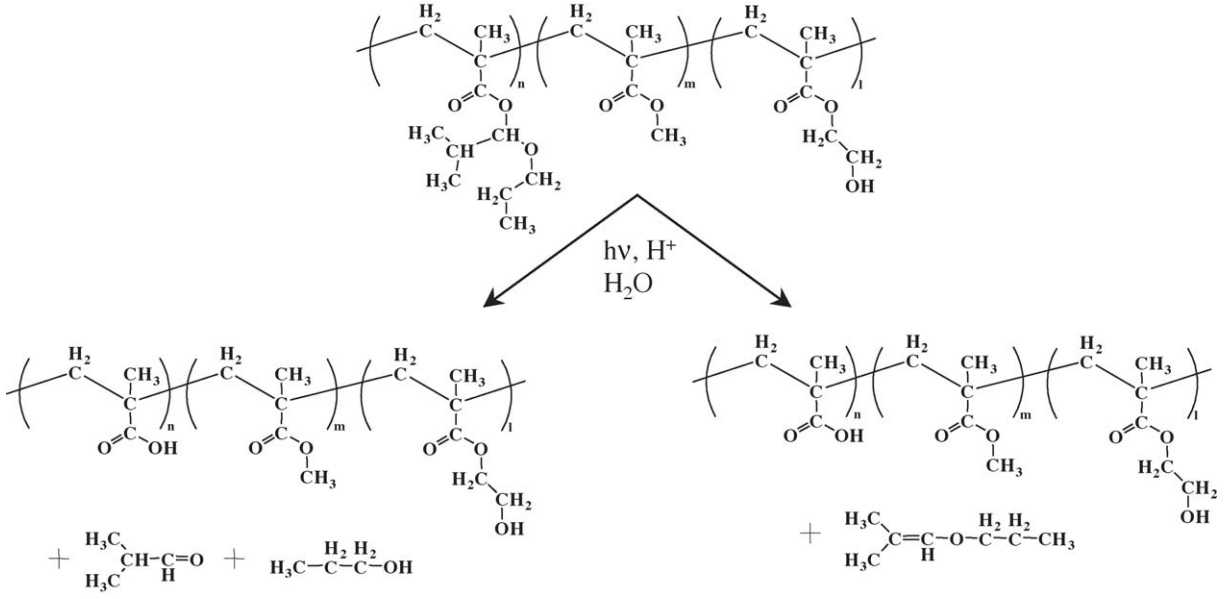


Scheme 3.

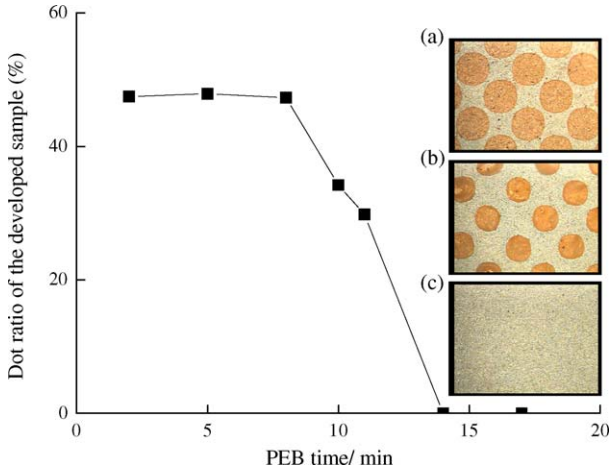


Fig. 8. Dot size of the developed sample dependence on the PEB time (65 lpi, 50%). Inset: dot photographs of the samples (a) 2 min, (b) 11 min, (c) 17 min. Exposure energy = 1.64 mJ/cm$^2$.

Fig. 9. Printing plate (200 lpi) obtained from the system EPP/NIOTf with P-8003 binder polymer. Experimental condition: exposure energy = 0.5 mJ/cm$^2$; PEB 2 min.

exposure energy, owing to the fact that an excess of the photogenerated acids affected the dots of the printing plate in the unexposed area. The post-exposure baking (PEB) time dependence on the dot size was then examined to study the effect of the acid diffusion as shown in Fig. 8. In this experiment, the dot ratio was fixed (65 lpi, 50%) and the PEB time was changed from 2 min to 17 min. When the PEB time was shorter, the dot size kept its original ratio. However, as the time became longer, the dot started shrinking and lastly, was no longer observed. It is considered that the excessive acid diffusion strongly affected the dots and induced their shrinkage. Finally, by controlling the amount of the acids and their diffusion, we obtained a fine printing plate with a high resolution (Fig. 9).

## 4. Conclusion

The sensitization mechanism for the pyrromethene dye/NIOTf system in acetonitrile was investigated. The fluorescence rate constants, the values of Gibbs free energy change, and the direct observation of the reaction intermediate by nanosecond laser flash photolysis enabled us to conclude that a singlet electron transfer from the pyrromethene derivative to NIOTf takes place in these systems. This photoinduced electron-transfer reaction appears as the primary process leading to the acid generation. The application of the EPP/NIOTf system to printing technology was performed and resulted in a fine printing plate with a high resolution (200 lpi).

## References

[1] B.M. Monroe, G.C. Weed, Chem. Rev. 93 (1993) 435.
[2] J.P. Fouassier, Photoinitiation, in: Photopolymerization and Photocuring, Hanser Publisher, New York, 1995.
[3] J.V. Crivello, K. Dietliker, Photoinitiators for Free Radical Cationic & Anionic Photopolymerisation, vol. III, second ed., John Wiley and Sons, New York, 1998.
[4] S. Suzuki, T. Urano, K. Ito, T. Murayama, I. Hotta, S. Takahara, T. Yamaoka, J. Photopolym. Sci. Tech. 17 (2004) 125.
[5] S. Noppakundilograt, S. Suzuki, T. Urano, N. Miyagawa, S. Takahara, T. Yamaoka, Polym. Adv. Technol. 13 (2002) 527.
[6] H. Ito, C.G. Willson, Polym. Eng. Sci. 23 (1982) 1012.
[7] H. Ito, C.G. Willson, J.M.J. Frechet, M.H. Farrall, E. Eichler, Macromolecules 16 (1983) 510.
[8] F. Ortica, J.C. Scaiano, G. Pohlers, J.F. Cameron, A. Zampini, Chem. Mater. 12 (2000) 414.
[9] G.M. Wallraff, R.D. Allen, W.D. Hinsberg, C.G. Willson, L.L. Simpson, S.E. Webber, J.L. Sturtevant, J. Imag. Tech. 36 (1992) 468.
[10] G. Pohlers, J.C. Scaiano, R. Sinta, Chem. Mater. 9 (1997) 3222.
[11] E. Leete, L. Marion, Can. J. Chem. 30 (1952) 563.
[12] M. Shah, K. Thangaraj, M.L. Soong, L.T. Wolford, J.H. Boyer, Heteroatom. Chem. 1 (1990) 389.
[13] G. Sathyamoorthi, J.H. Boyer, T.H. Allik, S. Chandra, Heteroatom. Chem. 5 (1994) 403.
[14] M. Wada, S. Ito, H. Uno, T. Murashima, N. Ono, T. Urano, Y. Urano, Tetrahedron Lett. 42 (2001) 6711.
[15] I. García-Moreno, A. Costela, L. Campo, R. Sastre, F. Amat-Guerri, M. Liras, F.L. Arbeloa, J.B. Prieto, I.L. Arbeloa, J. Phys. Chem. A 108 (2004) 3315.
[16] R.K. Kar, S.C. Bera, J. Photochem. Photobiol. A: Chem. 49 (1989) 121.
[17] A.A. Gorman, I. Hamblett, T.A. King, M.D. Rahn, J. Photochem. Photobiol. A: Chem. 130 (2000) 127.
[18] G. Jones II, S. Kumar, O. Klueva, D. Pacheco, J. Phys. Chem. A. 107 (2003) 8429.
[19] F.L. Arbeloa, T.A. Lopez, I.L. Arbeloa, J. Photochem. Photobiol. A: Chem. 121 (1999) 177.
[20] T.A. Lopez, F.L. Arbeloa, I.L. Arbeloa, I. García-Moreno, A. Costela, R. Sastre, F. Amat-Guerri, Chem. Phys. Lett. 299 (1999) 315.
[21] J.B. Prieto, F.L. Arbeloa, V.M. Martínez, T.A. Arbeloa, F. Amat-Guerri, M. Liras, I.L. Arbeloa, Chem. Phys. Lett. 385 (2004) 29.
[22] M.S. Mackey, W.N. Sisk, Dye Pigments 51 (2001) 79.
[23] W.N. Sisk, N. Ono, T. Yano, M. Wada, Dye Pigments 55 (2002) 143.
[24] S. Blaya, P. Acebal, L. Carretero, A. Fimia, Opt. Commun. 228 (2003) 55.
[25] J.M. Brom Jr., J.L. Langer, J. Alloys Comp. 338 (2002) 112.
[26] T. Urano, E.O. Okumura, K. Sakamoto, S. Suzuki, T. Yamaoka, N. Hara, K. Fukui, T. Karatsu, A. Kitamura, J. Photopolym. Sci. Tech. 13 (2000) 691.
[27] M. Shah, N.S. Allen, N.G. Salleh, T. Corrales, M. Egde, F. Catalina, P. Bosch, A. Green, J. Photochem. Photobiol. A: Chem. 111 (1997) 229.
[28] D. Rehm, A. Weller, Israel J. Chem. 8 (1970) 259.
[29] K. Okada, K. Okamoto, M. Oda, J. Am. Chem. Soc. 110 (1988) 8736.
[30] S.A. MacDonald, C.G. Willson, J.M. Frechet, Acc. Chem. Res. 27 (1994) 151.